



**Hall and Seebeck measurements estimate the thickness of a (buried) carrier system:  
Identifying interface electrons in In-doped SnO<sub>2</sub> films**

Alexandra Papadogianni, Mark E. White, James S. Speck, Zbigniew Galazka, and Oliver Bierwagen

Citation: [Applied Physics Letters](#) **107**, 252105 (2015); doi: 10.1063/1.4938471

View online: <http://dx.doi.org/10.1063/1.4938471>

View Table of Contents: <http://scitation.aip.org/content/aip/journal/apl/107/25?ver=pdfcov>

Published by the [AIP Publishing](#)

---

**Articles you may be interested in**

[Morphology, composition and electrical properties of SnO<sub>2</sub>:Cl thin films grown by atomic layer deposition](#)  
J. Vac. Sci. Technol. A **34**, 01A112 (2016); 10.1116/1.4933328

[The n-type conduction of indium-doped Cu<sub>2</sub>O thin films fabricated by direct current magnetron co-sputtering](#)  
Appl. Phys. Lett. **107**, 083901 (2015); 10.1063/1.4928527

[High electron mobility in epitaxial SnO<sub>2-x</sub> in semiconducting regime](#)  
APL Mater. **3**, 076107 (2015); 10.1063/1.4927470

[Limits of carrier mobility in Sb-doped SnO<sub>2</sub> conducting films deposited by reactive sputtering](#)  
APL Mater. **3**, 062802 (2015); 10.1063/1.4916586

[Electron transport properties of antimony doped Sn O 2 single crystalline thin films grown by plasma-assisted molecular beam epitaxy](#)  
J. Appl. Phys. **106**, 093704 (2009); 10.1063/1.3254241

---

A promotional banner for Applied Physics Reviews. On the left is a small image of the journal cover, which features a 3D diagram of a layered structure. The main text 'NEW Special Topic Sections' is in large white font on a blue background with a light flare. Below this, 'NOW ONLINE' is in yellow, followed by 'Lithium Niobate Properties and Applications: Reviews of Emerging Trends' in white. The AIP Applied Physics Reviews logo is in the bottom right corner.

**NEW Special Topic Sections**

**NOW ONLINE**  
Lithium Niobate Properties and Applications:  
Reviews of Emerging Trends

**AIP** Applied Physics  
Reviews

# Hall and Seebeck measurements estimate the thickness of a (buried) carrier system: Identifying interface electrons in In-doped SnO<sub>2</sub> films

Alexandra Papadogianni,<sup>1</sup> Mark E. White,<sup>2</sup> James S. Speck,<sup>2</sup> Zbigniew Galazka,<sup>3</sup> and Oliver Bierwagen<sup>1</sup>

<sup>1</sup>Paul-Drude-Institut für Festkörperelektronik, Hausvogteiplatz 5-7, D-10117 Berlin, Germany

<sup>2</sup>Materials Department, University of California, Santa Barbara, California 93106, USA

<sup>3</sup>Leibniz-Institut für Kristallzüchtung, Max-Born-Straße 2, D-12489 Berlin, Germany

(Received 14 October 2015; accepted 10 December 2015; published online 24 December 2015)

We propose a simple method based on the combination of Hall and Seebeck measurements to estimate the thickness of a carrier system within a semiconductor film. As an example, this method can distinguish “bulk” carriers, with homogeneous depth distribution, from “sheet” carriers, that are accumulated within a thin layer. The thickness of the carrier system is calculated as the ratio of the integral sheet carrier concentration, extracted from Hall measurements, to the volume carrier concentration, derived from the measured Seebeck coefficient of the same sample. For rutile SnO<sub>2</sub>, the necessary relation of Seebeck coefficient to volume electron concentration in the range of  $3 \times 10^{17}$  to  $3 \times 10^{20} \text{ cm}^{-3}$  has been experimentally obtained from a set of single crystalline thin films doped with varying Sb-doping concentrations and unintentionally doped bulk samples, and is given as a “calibration curve.” Using this calibration curve, our method demonstrates the presence of interface electrons in homogeneously deep-acceptor (In) doped SnO<sub>2</sub> films on sapphire substrates.

© 2015 AIP Publishing LLC. [<http://dx.doi.org/10.1063/1.4938471>]

The carrier concentration is a key property in semiconducting materials and devices for applications and materials characterization. Its depth distribution in semiconductor films can be vastly different by design or unintentionally, and is not necessarily known *a-priori*. For example, by doping the entire film, a homogeneous carrier concentration can be realized, whereas delta-doping or the use of (modulation) doped quantum wells can concentrate the carriers to a thin slice within the film. A rather unintentional charge concentration at the surface can result from surface Fermi level pinning within a band, e.g., for InN<sup>1-4</sup> or In<sub>2</sub>O<sub>3</sub>.<sup>5,6</sup> Similarly, unintentionally doped (UID) interface carriers can arise due to interfacial impurities, e.g., from InP substrates,<sup>7</sup> or the band-alignment of the film and the underlying substrate forming a triangular interfacial quantum well. Additionally, they can also be related to dislocations, e.g., in heteroepitaxial InN<sup>3</sup> or SnO<sub>2</sub> films,<sup>8-10</sup> used as example in this work.

Carrier concentrations are typically and conveniently determined by Hall effect measurements, which essentially integrate the volume carrier concentration over the entire thickness of the sample to provide a sheet Hall carrier concentration,  $n_{2d}^H$ . This measured  $n_{2d}^H$  is divided by the thickness of the carrier system to obtain the volume Hall carrier concentration,  $n_{3d}^H$ . The question that arises is which carrier system is actually represented by the Hall measurements, as the typical assumption that carriers are evenly distributed across the entire film thickness (“bulk carriers”) may be misleading as described by the above scenarios and with our SnO<sub>2</sub> example later.

Carrier concentration profiling methods can resolve this issue but have their own drawbacks: For example, capacitance-voltage (CV) profiling directly measures the volume carrier concentration profile, but is typically limited to the near-surface region and requires the formation of Schottky

contacts. Significantly more effort is required for extending the profiling range to the entire sample thickness by Hall profiling using the differential Hall effect technique by either successive stripping of layers<sup>11,12</sup> or analyzing a series of samples with different thickness,<sup>3,10</sup> also used to determine the unintentional donor concentration profile in our SnO<sub>2</sub> films for reference.

An easily measured but significant thermoelectric property is the Seebeck coefficient  $S$ , which is the voltage divided by its inducing temperature difference across a semiconductor.<sup>13</sup> Its sign indicates the dominant carrier type in a material (positive  $S$  for *p*-type and negative for *n*-type), which has been utilized to demonstrate *p*-type carriers in cases where Hall measurements failed due to either parallel *n*-type carrier systems in InN<sup>4,14</sup> or too low mobility in the transparent conducting oxide Sr-doped LaCrO<sub>3</sub>.<sup>15</sup> We will also use it here to demonstrate *n*-type conductivity in our In-doped SnO<sub>2</sub> films. The direct relation to the Fermi level makes  $S$  dependent on the volume carrier concentration,<sup>13</sup> which has been utilized, for example, to determine the volume electron concentration in InAs nanowires<sup>16</sup> or the hole concentration in Sr-doped LaCrO<sub>3</sub><sup>15</sup> from the measured Seebeck coefficient. Examples for the required relation of  $S$  to the volume carrier concentration  $n_{3d}$  in different materials are theoretically modeled calibration curves for InAs,<sup>16</sup> InN,<sup>17</sup> Sr-doped LaCrO<sub>3</sub>,<sup>15</sup> and In<sub>2</sub>O<sub>3</sub>,<sup>18</sup> or experimentally obtained calibration curves for InN<sup>3,4</sup> and In<sub>2</sub>O<sub>3</sub>.<sup>18</sup>

In the present study, we propose how the comparably simple combination of the Seebeck coefficient and Hall effect measurements can be used to estimate the thickness of a carrier system, and thus distinguish bulk from sheet carriers. Essentially, the integral sheet carrier concentration from Hall measurements,  $n_{2d}^H$ , divided by the volume carrier concentration derived from the Seebeck coefficient,  $n_{3d}^S$ , is used as an estimate of the carrier system’s thickness  $t_c$ .

$$t_c = n_{2d}^H / n_{3d}^S. \quad (1)$$

After experimentally determining the calibration curve,  $S(n_{3d})$ , for SnO<sub>2</sub> over an electron-concentration range of  $3 \times 10^{17}$  to  $3 \times 10^{20} \text{ cm}^{-3}$ , we demonstrate how our method can identify a thin interface carrier system in SnO<sub>2</sub> films homogeneously doped with the deep acceptor indium. This carrier system is shown to arise from a large unintentional donor concentration at the film–substrate interface, which could not be completely compensated by the deep acceptors.

Fig. 1 schematically shows the samples used for this study. For the measurement of  $S(n_{3d})$ , high-quality single crystalline rutile epitaxial Sb-doped SnO<sub>2</sub> thin films were grown by plasma-assisted molecular beam epitaxy (PA-MBE)<sup>8,19</sup> on *r*-plane Al<sub>2</sub>O<sub>3</sub> substrates with electron concentrations in the range of  $7 \times 10^{17}$  to  $3 \times 10^{20} \text{ cm}^{-3}$ . In our SnO<sub>2</sub> thin film samples, a high UID electron concentration has been identified at the interface to the Al<sub>2</sub>O<sub>3</sub> substrate,<sup>8–10</sup> also shown later. To decouple the Sb-doping from this interface region, the Sb-doped thin films consist of the 545 nm-thick homogeneously Sb-doped layer on top of a 545 nm-thick UID buffer layer (Fig. 1(a)). As a reference, a 545 nm-thick UID buffer layer, fully containing the interface region, was grown without Sb-doped layer on top (Fig. 1(b)). Lower electron concentrations from  $3 \times 10^{17}$  to  $1 \times 10^{18} \text{ cm}^{-3}$  for our calibration curve were provided by approximately 800  $\mu\text{m}$ -thick UID rutile bulk SnO<sub>2</sub> samples grown by the physical vapor transport<sup>20</sup> (Fig. 1(c)). A series of rutile UID SnO<sub>2</sub> films on *r*-plane Al<sub>2</sub>O<sub>3</sub> substrates with varying thickness in the range of 26–1570 nm (Fig. 1(d)) was grown to study the UID concentration profile, which peaks at the substrate interface. Finally, as samples with a thin carrier system,  $\approx 440$  and  $\approx 1200$  nm-thick rutile SnO<sub>2</sub> films were grown by PA-MBE that are homogeneously doped with the deep acceptor indium (Fig. 1(e)).<sup>21</sup> As will be shown, the indium fully compensates the UID donors in the film except for the interface region. The Sb- and In-concentrations in the films were measured by calibrated secondary ion mass spectrometry.<sup>8,21</sup>

Room temperature (RT) Hall measurements in ambient atmosphere were performed with all samples using the vander-Pauw technique on approx. 7 mm  $\times$  7 mm large square shaped sample pieces with small indium contacts in the corners. The RT Seebeck coefficient of all samples was measured in ambient atmosphere as described in detail in Ref. 18.

Due to the dual-layer character of the Sb-doped films, the transport properties (Hall and Seebeck) of the Sb-doped layer were extracted using a dual-layer approach, by “subtracting” the transport properties of the underlying (reference) buffer

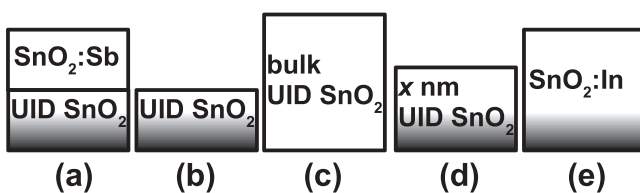


FIG. 1. Schematics of thin films (a), (b), (d), and (e) and bulk samples (c) used in this study. The dark gradient at the bottom of the thin films symbolizes the UID interface donors.

layer (Fig. 1(b)) from that of the Sb-doped films (Fig. 1(a)) as described in Ref. 3. The extracted sheet electron concentration of the homogeneously Sb-doped layer was divided by its thickness to calculate its volume electron concentration, and the sheet electron concentration measured for the bulk samples was divided by their thickness. The Hall-profiling methodology described in Ref. 3 was also used with the UID thickness series (Fig. 1(d)) to determine the profile of the unintentional donor concentration close to the SnO<sub>2</sub>–Al<sub>2</sub>O<sub>3</sub> interface.

The acquired Seebeck coefficient of the Sb-doped layers and the bulk samples, as well as the available literature data are compiled into Fig. 2 as a function of volume electron concentration. (Note that, due to unknown Hall scattering factor, we assume the electron concentration to be identical to the electron concentration measured by the Hall effect.) A calibration curve (red solid line) has been roughly adjusted to the obtained data and can be used to estimate  $n_{3d}$  from Seebeck coefficient  $S$  of any SnO<sub>2</sub> sample. The approximate error bar in the figure indicates that the electron concentration can be estimated within a factor of two uncertainty.

Fig. 2 further depicts a simplified analytical modeling of the Seebeck coefficient as a function of both non-degenerate and degenerate volume electron concentrations<sup>13</sup> that is detailed in Ref. 18. A density-of-states effective electron mass of 0.275 times the free electron mass<sup>27</sup> and Seebeck scattering parameters  $r$  for the two limiting scattering mechanisms ionized impurity scattering ( $r=1.5$ ) and the polar optical phonon ( $r=0.5$ ) were considered. The boundary between the non-degenerate and degenerate volume carrier

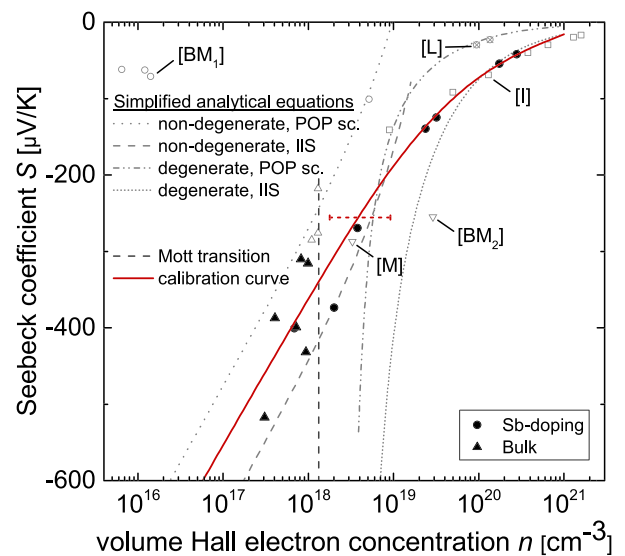


FIG. 2. Seebeck coefficient as a function of volume electron concentration determined by Hall effect measurements for SnO<sub>2</sub>. Data are shown for our own Sn-doped films and UID bulk samples. Published data from the literature are included: [BM<sub>1</sub>] Bagheri-Mohagheghi and Shokooh-Saremi,<sup>22</sup> [BM<sub>2</sub>] Bagheri-Mohagheghi *et al.*,<sup>23</sup> [I] Islam and Hakim,<sup>24</sup> [L] Lang and Li,<sup>25</sup> and [M] Moharrami *et al.*<sup>26</sup> Broken lines represent the modeling based upon simplified analytical equations for the degenerate and non-degenerate cases and the limiting polar optical phonon (POP) and ionized impurity (IIS) scattering. The broken, vertical line denotes the calculated Mott transition from non-degenerate to degenerate behavior. The red, solid curve is an empirical fit to the data in order to approximately describe the Seebeck coefficient of SnO<sub>2</sub> as a function of volume electron concentration. The horizontal error bar represents the uncertainty of our empirical fit.

TABLE I. Properties of the homogeneously In-doped SnO<sub>2</sub> samples.  $N_{In}$  is the indium concentration as measured by calibrated secondary ion mass spectrometry,  $R_S$  and  $n_{2d}^H$  the as measured sheet resistance and sheet electron concentration by the van-der-Pauw Hall method,  $n_{3d}^H = n_{2d}^H/t_f$  the corresponding calculated volume Hall electron concentration using film thickness  $t_f$  and assuming homogenous carrier distribution,  $S$  is the measured Seebeck coefficient,  $n_{3d}^S$  the volume electron concentration derived from  $S$  using our calibration curve (see Fig. 3), and  $t_c$  is the calculated thickness of the conductive layer using Eq. (1). For comparison with  $t_c$ , the thickness of the region of uncompensated UID donors at the interface  $d_u$  (see Fig. 4) is given.

Sample	$N_{In}$ (cm <sup>-3</sup> )	$R_{sheet}$ (kΩ/□)	$S$ (μV/K)	$n_{2d}^H$ (cm <sup>-2</sup> )	$n_{3d}^H$ (cm <sup>-3</sup> )	$n_{3d}^S$ (cm <sup>-3</sup> )	$t_c$ (nm)	$t_f$ (nm)	$d_u$ (nm)
S1	$4.5 \times 10^{18}$	87	-165	$3.1 \times 10^{13}$	$7.2 \times 10^{17}$	$1.5 \times 10^{19}$	22	437	33
S2	$2.8 \times 10^{18}$	138	-208	$2.2 \times 10^{13}$	$1.9 \times 10^{17}$	$7.4 \times 10^{18}$	29	1170	49
S3	$2.4 \times 10^{19}$	910	-167	...	...	$1.4 \times 10^{19}$	...	448	...

concentration region is determined by the Mott criterion,<sup>28</sup> which using a dielectric constant of 12.3 (Ref. 29) is at  $1.32 \times 10^{18} \text{ cm}^{-3}$ .

The fact that our measured data in Fig. 2 are well described within the boundaries of the simplified analytical curves for the two prominent scattering mechanisms and are qualitatively following the trend of the related semiconducting oxide In<sub>2</sub>O<sub>3</sub> (cf. Fig. 9 in Ref. 18) indicates that the electrons in these SnO<sub>2</sub> samples are indeed homogeneously distributed “bulk” carriers. In contrast, the strongly deviating data points “BM-1,” “BM-2,” and “L” in Fig. 2 are an indication of inhomogeneously distributed carriers.

We now apply our method and the determined calibration curve to estimate the carrier system thickness in epitaxially well-defined SnO<sub>2</sub> samples that have undergone homogenous indium-doping (Fig. 1(e)). Substituting Sn with In should either produce compensating acceptors if In acts as a deep acceptor—the amount of energy  $E_a$  to ionize the acceptors is large—or holes if In acts as a shallow acceptor— $E_a$  is small. Shallow acceptors can also be compensating, though, since any acceptor firstly compensates present donors. If the acceptor concentration  $N_A$  is greater than the donor concentration  $N_D$ , the remaining acceptors would then produce holes if shallow. Table I summarizes the Hall and Seebeck data of three homogeneously In-doped SnO<sub>2</sub> films. Both Hall and Seebeck measurements confirm that none of the In-doped samples exhibit *p*-type conductivity, in line with recent theoretical works that suggest polaronic hole localization<sup>30,31</sup> to result in effectively deep acceptors ( $E_a \simeq 580 \text{ meV}$ ). (A too low mobility explains why Hall measurements fail for the highest In-doped sample (Table I, S3) while the sheet resistance and Seebeck measurements are still functional.) The extraction of volume electron concentration from the calibration curve is graphically represented in Fig. 3 with the example of sample S1. The discrepancy of volume electron concentration derived from Hall measurements (assuming homogeneous carrier distribution) and Seebeck measurements for samples S1 and S2 is apparent in the figure and clearly indicates a concentration of the electron in a thin layer. The thickness of this layer,  $t_c$ , given in Table I has been calculated using Eq. (1) and is significantly lower than that of the entire film  $t_f$ .

This concentration of electrons in a thin layer can be understood as the interplay between a high donor concentration localized at the film–substrate interface<sup>8–10</sup> and the compensating effect of the homogeneous acceptor doping as schematically shown in Fig. 4: The high UID donor concentration at the interface between substrate and film (at  $d=0$ ) strongly

decreases with increasing distance to this interface, as determined by Hall profiling of the UID thickness series (Fig. 1(d)) and indicated by the black solid curve. Consequently, indium can fully compensate the low concentration UID donors in the bulk of the sample, but leaves a thin region of uncompensated high concentration UID donors near the interface, i.e., where  $N_D > N_A$ . The electrons from these uncompensated UID donors are the source of the electrical conductivity in our In-doped samples. (Their low mobility is related to the high dislocation density<sup>10</sup> and the additional high degree of compensation.) Quantitative comparison of the homogenous acceptor concentration to the UID donor concentrations profile indicated in Fig. 4 yields the thickness  $d_u$  of the interface region containing uncompensated donors for samples S1 and S2. Comparison of  $d_u$  with the carrier system thickness  $t_c$  extracted by our method shows a good agreement as seen in Table I. (While, in principle, a surface electron accumulation could contribute to the measured n-type conductivity, this possibility was ruled-out by analyzing films with higher doping in the interface region but moderate In-doping in the bulk region that turned semi-insulating.<sup>9</sup>)

The above example clearly demonstrated the validity of our method in the presence of one (dominating) carrier

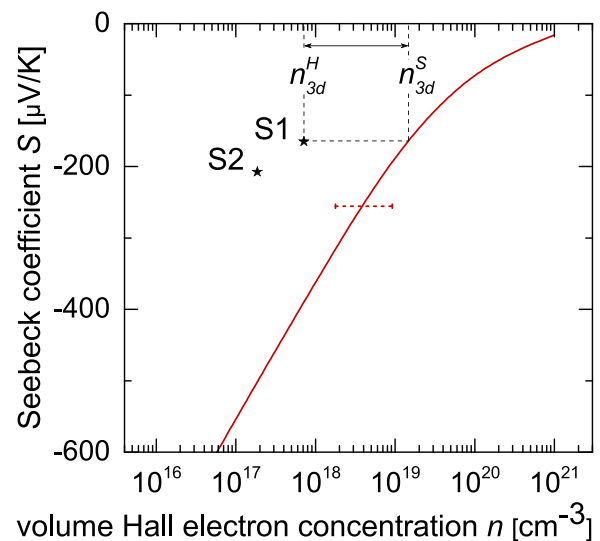


FIG. 3. Seebeck coefficient  $S$  and Hall volume electron concentration  $n_{3d}^H$  (assuming homogenous electron distribution) of homogeneously In-doped SnO<sub>2</sub> films S1 and S2. The red solid curve represents our empirical relation of Seebeck coefficient to volume electron concentration for SnO<sub>2</sub>. With the example of S1, the broken lines visualize how the volume electron concentration  $n_{3d}^S$  is determined from  $S$ . The arrow indicates the stark contrast of  $n_{3d}^S$  and the corresponding  $n_{3d}^H$ .

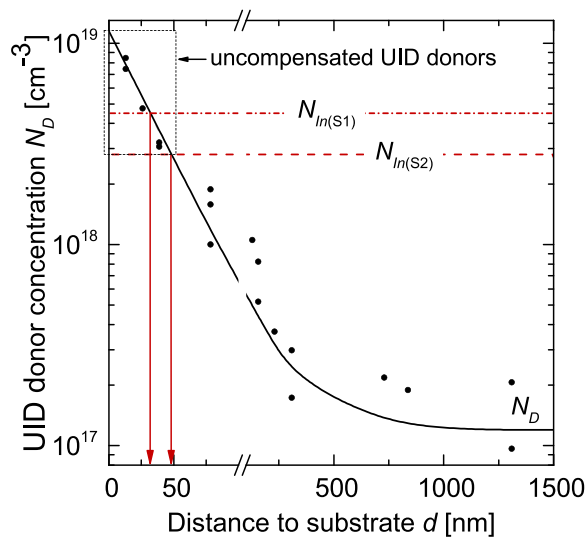


FIG. 4. Dopant concentrations in our In-doped SnO<sub>2</sub> films. Homogeneous acceptor concentration (red, dashed horizontal line) and UID donor concentration (data points and black, solid line as guide to the eye) with accumulation towards the interface as a function of distance to the film–substrate interface. Indium doping reduces the electron concentration of SnO<sub>2</sub> by compensating the UID donors but leaves a thin sheet of uncompensated UID donors close to the interface. The vertical, red, dashed lines indicate the distances  $d_u$  at which the acceptor concentration starts fully compensating the UID donor concentration (=thickness of layer with uncompensated UID donors) for samples S1 (33 nm) and S2 (49 nm).

system. If more carrier systems are present (electrons and holes simultaneously present in the same region, or different layers contributing to transport), they contribute to an apparent Seebeck coefficient  $S$  and sheet Hall electron concentration  $n_{2d}^H$  as described in Ref. 3. In this case the carrier system's thickness extracted by our method generally does not reflect the sum of their thicknesses. Notwithstanding, a carrier system's thickness strongly differing from the film thickness,  $t_c \neq t_f$ , is a generally sufficient criterion to indicate an inhomogeneous carrier distribution, whereas  $t_c = t_f$  is a necessary (but strictly speaking not sufficient) criterion to indicate a homogeneous carrier distribution.

To summarize, real-life semiconductor film samples can have a (unexpected) charge accumulation at surfaces or interfaces. This accumulation cannot be resolved by Hall measurements, which only determine an integral sheet carrier concentration. The Seebeck coefficient is a fundamental thermoelectric transport property, whose magnitude is related to the volume carrier concentration. Our proposed method of dividing the sheet carrier concentration from Hall measurements by the volume carrier concentration derived from Seebeck measurements can be used to estimate the thickness of a carrier system of any semiconducting material that allows Hall measurements, has a known carrier-concentration dependence of the Seebeck coefficient, and has one transport-dominating carrier system. For the transparent semiconducting oxide SnO<sub>2</sub> we provided such an experimental dependence in the volume electron concentrations range of  $3 \times 10^{17}$  to  $3 \times 10^{20} \text{ cm}^{-3}$  as “calibration curve.” The physical validity of this curve was shown, which in turn confirms the homogeneous electron concentration in the samples used to establish the calibration curve. We further validated our method with the example of SnO<sub>2</sub> films homogeneously doped with the deep

acceptor indium, which compensates the unintentional donors. Despite the homogeneous In-doping, the determined thickness of the electron system in these samples was significantly lower than that of the entire film, clearly indicating carrier accumulation rather than homogeneous distribution. Our qualitative and quantitative results in this example showed that this carrier accumulation was due to a high concentration of uncompensated unintentional donors at the film–substrate interface.

We would like to thank Y. Takagaki for critically reading the manuscript. A.P. was supported by DFG Grant No. BI 1754/1-1.

- <sup>1</sup>H. Lu, W. J. Schaff, L. F. Eastman, and C. E. Stutz, *Appl. Phys. Lett.* **82**, 1736 (2003).
- <sup>2</sup>T. Nagata, G. Koblmüller, O. Bierwagen, C. S. Gallinat, and J. S. Speck, *Appl. Phys. Lett.* **95**, 132104 (2009).
- <sup>3</sup>O. Bierwagen, S. Choi, and J. S. Speck, *Phys. Rev. B* **84**, 235302 (2011).
- <sup>4</sup>O. Bierwagen, S. Choi, and J. S. Speck, *Phys. Rev. B* **85**, 165205 (2012).
- <sup>5</sup>P. D. C. King, T. D. Veal, D. J. Payne, A. Bourlange, R. G. Egdell, and C. F. McConville, *Phys. Rev. Lett.* **101**, 116808 (2008).
- <sup>6</sup>O. Bierwagen, J. S. Speck, T. Nagata, T. Chikyow, Y. Yamashita, H. Yoshikawa, and K. Kobayashi, *Appl. Phys. Lett.* **98**, 172101 (2011).
- <sup>7</sup>K. Rakennus, K. Tappura, T. Hakkarainen, H. Asonen, R. Laiho, S. J. Rolfe, and J. J. Dubowski, *J. Cryst. Growth* **110**, 910 (1991).
- <sup>8</sup>M. E. White, O. Bierwagen, M. Y. Tsai, and J. S. Speck, *J. Appl. Phys.* **106**, 093704 (2009).
- <sup>9</sup>O. Bierwagen, T. Nagata, M. E. White, M.-Y. Tsai, and J. S. Speck, *J. Mater. Res.* **27**, 2232 (2012).
- <sup>10</sup>S. K. Vasheghani Farahani, T. D. Veal, A. M. Sanchez, O. Bierwagen, M. E. White, S. Gorfman, P. A. Thomas, J. S. Speck, and C. F. McConville, *Phys. Rev. B* **86**, 245315 (2012).
- <sup>11</sup>R. Baron, G. A. Shifrin, O. J. Marsh, and J. W. Mayer, *J. Appl. Phys.* **40**, 3702 (1969).
- <sup>12</sup>S. R. Blight, R. E. Nicholls, S. P. S. Sangha, P. B. Kirby, L. Teale, S. P. Hiscock, and C. P. Stewart, *J. Phys. E: Sci. Instrum.* **21**, 470 (1988).
- <sup>13</sup>K. Seeger, *Semiconductor Physics*, 9th ed. (Springer, 2004).
- <sup>14</sup>L. H. Dmowski, M. Baj, T. Suski, J. Przybytek, R. Czernecki, X. Wang, A. Yoshikawa, H. Lu, W. J. Schaff, D. Muto, and Y. Nanishi, *J. Appl. Phys.* **105**, 123713 (2009).
- <sup>15</sup>K. H. L. Zhang, Y. Du, A. Papadogianni, O. Bierwagen, S. Sallis, L. F. J. Piper, M. E. Bowden, V. Shutthanandan, P. V. Sushko, and S. A. Chambers, *Adv. Mater.* **27**, 5191 (2015).
- <sup>16</sup>V. Schmidt, P. F. J. Mensch, S. F. Karg, B. Gotsmann, P. Das Kanungo, H. Schmid, and H. Riel, *Appl. Phys. Lett.* **104**, 012113 (2014).
- <sup>17</sup>N. Miller, J. W. Ager III, H. M. Smith III, M. A. Mayer, K. M. Yu, E. E. Haller, W. Walukiewicz, W. J. Schaff, C. S. Gallinat, G. Koblmüller, and J. S. Speck, *J. Appl. Phys.* **107**, 113712 (2010).
- <sup>18</sup>N. Preissler, O. Bierwagen, A. T. Ramu, and J. S. Speck, *Phys. Rev. B* **88**, 085305 (2013).
- <sup>19</sup>M. E. White, M. Y. Tsai, F. Wu, and J. S. Speck, *J. Vac. Sci. Technol., A* **26**, 1300 (2008).
- <sup>20</sup>Z. Galazka, R. Uecker, D. Klimm, K. Imscher, M. Pietsch, R. Schewski, M. Albrecht, A. Kwasiński, S. Ganschow, D. Schulz, C. Guguschev, R. Bertram, M. Bickermann, and R. Fornari, *Phys. Status Solidi A* **211**, 66 (2014).
- <sup>21</sup>M. E. White, O. Bierwagen, M.-Y. Tsai, and J. S. Speck, *Appl. Phys. Express* **3**, 051101 (2010).
- <sup>22</sup>M.-M. Bagheri-Mohagheghi and M. Shokooh-Saremi, *Physica B* **405**, 4205 (2010).
- <sup>23</sup>M.-M. Bagheri-Mohagheghi, N. Shahtahmasebi, M. Alinejad, A. Youssefi, and M. Shokooh-Saremi, *Solid State Sci.* **11**, 233 (2009).
- <sup>24</sup>M. N. Islam and M. O. Hakim, *J. Phys. D: Appl. Phys.* **18**, 71 (1985).
- <sup>25</sup>W.-J. Lang and Z.-Q. Li, *Appl. Phys. Lett.* **105**, 042110 (2014).
- <sup>26</sup>F. Moharrami, M.-M. Bagheri-Mohagheghi, H. Azimi-Juybari, and M. Shokooh-Saremi, *Phys. Scr.* **85**, 015703 (2012).
- <sup>27</sup>K. J. Button, C. G. Fonstad, and W. Dreybrodt, *Phys. Rev. B* **4**, 4539 (1971).
- <sup>28</sup>N. Mott, *Proc. R. Soc. London, Ser. A* **382**, 1 (1982).
- <sup>29</sup>A. Schleife, J. B. Varley, F. Fuchs, C. Rödl, F. Bechstedt, P. Rinke, A. Janotti, and C. G. Van de Walle, *Phys. Rev. B* **83**, 035116 (2011).
- <sup>30</sup>S. Lany and A. Zunger, *Phys. Rev. B* **80**, 085202 (2009).
- <sup>31</sup>J. B. Varley, A. Janotti, C. Franchini, and C. G. Van de Walle, *Phys. Rev. B* **85**, 081109 (2012).